Simultaneous measurements of high-frequency pump-enhanced airglow and ionospheric temperatures at auroral latitudes

T. B. Leyser[1], B. Gustavsson[2], B. U. E. Brändström[2], Å. Steen[2],
F. Honary[3], M. T. Rietveld[4], T. Aso[5] and M. Ejiri[5]

[1]*Swedish Institute of Space Physics, Uppsala Division, S-755 91 Uppsala, Sweden*
[2]*Swedish Institute of Space Physics, Kiruna Division, P. O. Box 812, S-981 28 Kiruna, Sweden*
[3]*Department of Communication Systems, Lancaster University, Lancaster LA1 4YR, U. K.*
[4]*European Incoherent Scatter Association, N-9027 Ramfjordbotn, Norway*
[5]*National Institute of Polar Research, Arctic Environment Research Center, Kaga 1-chome,
Itabashi-ku, Tokyo 173-8515*

Abstract: Simultaneous measurements of enhanced airglow at 6300 Å and plasma temperatures from transmitting a powerful high frequency electromagnetic pump wave from the EISCAT-Heating facility into the ionospheric F region at auroral latitudes are reported. The airglow was detected with the Auroral Large Imaging System in northern Sweden and the background plasma parameter values were obtained with the EISCAT-UHF incoherent scatter radar. The multi-station imaging technique enables triangulation of the height and position of the enhanced airglow volume. By using a tomography inversion technique it is found that the shape of the airglow cloud is roughly spherical but varies. Further, the airglow enhancement is correlated with large pump-induced electron temperature enhancements of up to 250%. These temperature enhancements extend several hundred kilometers above and several tens of kilometers below the airglow cloud.

1. Introduction

A powerful high frequency (HF) electromagnetic pump wave transmitted into the ionosphere from the ground may excite plasma processes on a wide range of temporal and spatial scales. One purpose of such experiments is to study the response of the plasma to externally imposed energy flux. Interesting self organization in response to the HF pumping occurs when short time scale ponderomotive turbulence interacts with slow transport type processes, which leads to, *e.g.*, the occurrence of filamentary density structures stretched along the geomagnetic field, anomalous heating, and stimulated electromagnetic emissions. The topic of the present treatment is that of enhanced airglow by HF pumping, which has been observed during nighttime. Pump-enhanced airglow has been studied at mid latitudes at Platteville, U.S.A. (Sipler and Biondi, 1972; Haslett and Megill, 1974), Arecibo, Puerto Rico (Sipler *et al.*, 1974; Carlson *et al.*, 1982; Bernhardt *et al.*, 1989b), Moscow, Russia (Adeishvili *et al.*, 1978), Sura, Russia (Bernhardt *et al.*, 1991), and at the auroral latitude of Tromsø, Norway (Brändström *et al.*, 1999). The present report concerns measurements of enhanced airglow using facilities of the European Incoherent Scatter Association (EISCAT) in Ramfjordmoen at auroral latitudes

in northern Norway together with the Auroral Large Imaging System (ALIS) in northern Sweden. Initial results from the experiments have been presented by Brändström *et al.* (1999). Here we present further analysis of the airglow data together with simultaneously measured plasma parameter values such as the electron and ion temperatures.

Studies of enhanced airglow are useful to understand electron energization during driven plasma turbulence, *e.g.*, what the roles of heating, on the one hand, and electron acceleration, on the other hand, are for dissipating the turbulence. Both heating and electron acceleration are common phenomena in plasma and space physics and occur during a variety of conditions. Airglow enhancement typically occurs as a result of excitation of the $O(^1D)$ meta-stable state, which radiates at 6300 Å (the red line) as the oxygen atom relaxes to its ground state again. The $O(^1D)$ state is excited by inelastic collisions with electrons having energies above 1.96 eV (Rees, 1989). However, electrons with energies of 2–3.5 eV excite vibrational states in N_2, so that the effective threshold to excite the $O(^1D)$ state in the thermosphere is approximately 3.5 eV (Haslett and Megill, 1974; Bernhardt *et al.*, 1991). The next excited state in atomic oxygen is the $O(^1S)$ state, which radiates at 5577 Å (the green line) and is excited by electrons having energies of 4.17 eV or more (Haslett and Megill, 1974 ; Rees, 1989). The present treatment concerns observations of the red line.

Basically two different hypotheses have been suggested for excitation of the electrons which are necessary to observe enhanced airglow. In the first case it is assumed that the electron velocity distribution remains essentially Maxwellian during the pumping. The energetic electrons are associated with the tail of the velocity distribution of the pump-enhanced electron temperature (Mantas, 1994; Mantas and Carlson, 1996; Gurevich and Milikh, 1997). In the second case the supra-thermal electrons belong to a non-Maxwellian distribution, which results from acceleration processes in Langmuir turbulence driven by the pump wave (Perkins and Kaw, 1971; Haslett and Megill, 1974; Sipler *et al.*, 1974; Weinstock, 1975; Gurevich *et al.*, 1985).

2. Experimental facilities

The results were obtained on 16 February 1999 by using the EISCAT-Heating facility (Rietveld *et al.*, 1993) as the transmitter of a powerful electromagnetic HF pump wave. The pump wave was transmitted in ordinary mode at a frequency of 4.04 MHz such that it reflected in the ionospheric *F* region. The effective radiated power (ERP) was approximately 125 MW and the pump beam was tilted 6° south from the vertical, which is approximately half the angle between the vertical and the geomagnetic field in the *F* region above the Heating facility. HF pump experiments at the high latitudes of EISCAT-Heating facilitate strong excitation of plasma turbulence in a wide range of angles to the geomagnetic field, since the pump electric field is directed parallel to the geomagnetic field at the reflection height and essentially perpendicular to the magnetic field at only a few kilometers lower altitude (Leyser, 1991).

The EISCAT-UHF incoherent scatter radar at a frequency of approximately 930 MHz was used to measure background plasma parameter values. The UHF radar was operating in the Common-Programme-1 mode with a GEN-type long pulse and alternating code (Wannberg, 1993) and was directed parallel to the geomagnetic field.

The data presented below was obtained from the long pulse, which gives a range resolution of 22.5 km. With a UHF radar beam width of approximately 3 km at the pump–plasma interaction height, the radar scatter occurs only from a very small volume of the interaction region which has an horizontal extent of the order of 50 km.

ALIS is a weak-light imaging facility in the Kiruna area in northern Sweden (Steen and Brändström, 1993). As shown in Fig. 1, it consists of six remote controlled stations, each with a non-intensified charge-coupled-device (CCD) camera with 1024×1024 pixels and 16 bits/pixel. For the measurements reported here the sensitivity of the CCD cameras was enhanced by a factor of 64 by on-chip binning 8×8 pixels, thereby reducing the resolution to 128×128 pixels. Since the CCD cameras have not been calibrated the intensity data is plotted in raw counts below. ALIS operated with 10-s image interval and 5-s integration time of emissions at 6300 Å.
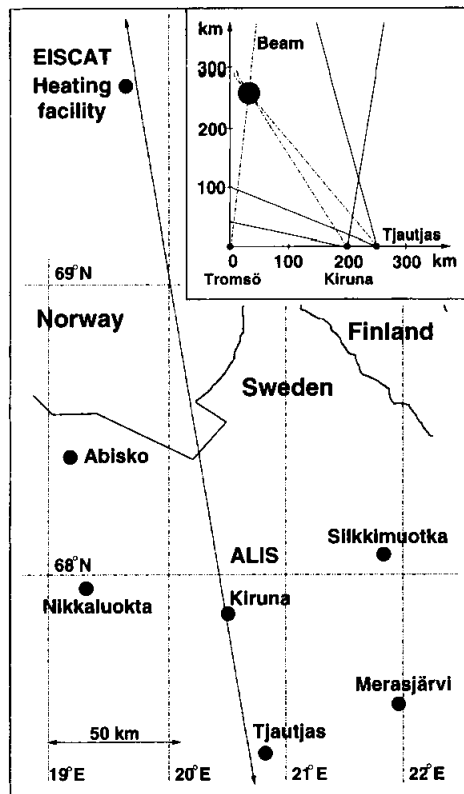

Fig. 1. Schematic diagram of ALIS in the Kiruna area in northern Sweden (from Brändström et al., 1999). The insert illustrates a vertical cut along the Kiruna-Tromsø meridian. The bullet indicates the anticipated region of enhanced airglow and the solid lines shows the field of view of the cameras.

3. Experimental results

The pump wave was cycled 2 min on/2 min off between 1632–1722 UT and 4 min on/4 min off between 1724–1832 UT. As the pump was cycled 2 min on/2 min off weakly enhanced airglow was detected during the pumping. Between 1732–1830 UT as the pump was cycled 4 min on/4 min off, significantly enhanced airglow was detected by all ALIS stations in operation. Figure 2 shows time series of the maximum intensity of
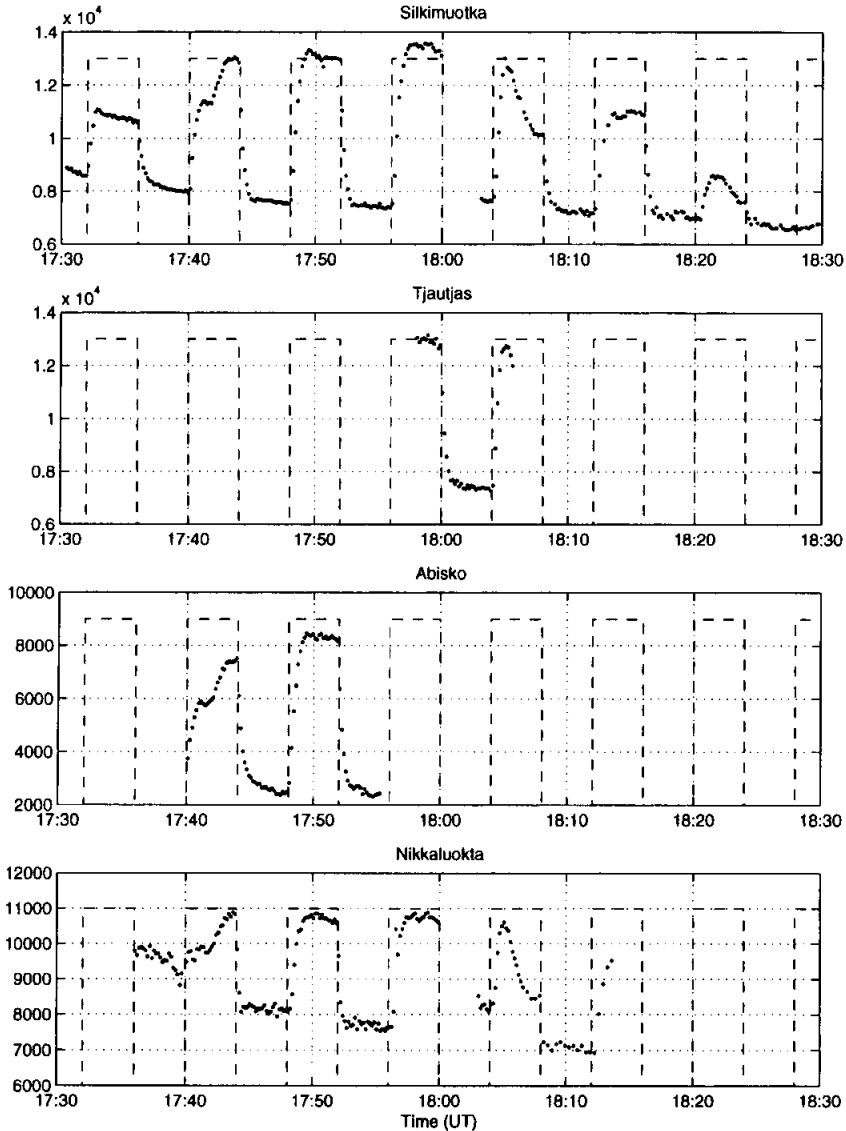

Fig. 2. Temporal evolution of enhanced airglow as observed from the Silkkimuotka (top), Tjautjas, Abisko, and Nikkaluokta (bottom) stations (from Brändström et al., 1999). Each dot represents the maximum intensity in the corresponding image (in raw counts). The dashed square wave indicates the pump cycle.

the 6300-Å emissions *versus* time from the four observing stations. The airglow intensity grows with an *e*-folding growth time of approximately 60 s after pump-on and decays with an *e*-folding decay time of approximately 35 s after pump-off. Also, following the growth phase after pump-on, the maximum emission intensity exhibits different temporal evolution at different pump periods. The occasional data losses are due to clouds or technical problems.

Figure 3 displays a series of images of the airglow near pump-on and -off obtained from the Silkkimuotka station for the pump period 1748–1752 UT. The airglow intensity and size of the patch is seen to increase slowly after pump-on and decrease slowly after pump-off.

As the enhanced airglow was detected by up to three stations simultaneously (Fig. 2), triangulation of the height of the airglow volume and estimates of the volume extent is possible. The typical height of the maximum emission is found to be approximately 240 km, which is slightly lower than the pump reflection height of approximately 250 km as obtained from the Dynasonde and EISCAT-UHF radar. Results of tomography inversion gives that the shape of the enhanced airglow excitation region is roughly spherical but varies slightly from pump pulse to pulse. After correction for diffusion and the long life time of 110 s of the $O(^1D)$ state, the excitation region is found to have an *e*-folding scale length of the order of 10 km. Detailed discussion of the tomography inversion technique and its results for the present experiments will be presented elsewhere.

Figure 4 shows background plasma parameter values versus height and time between 1724–1828 UT as obtained from the EISCAT-UHF radar. In Fig. 4a the electron
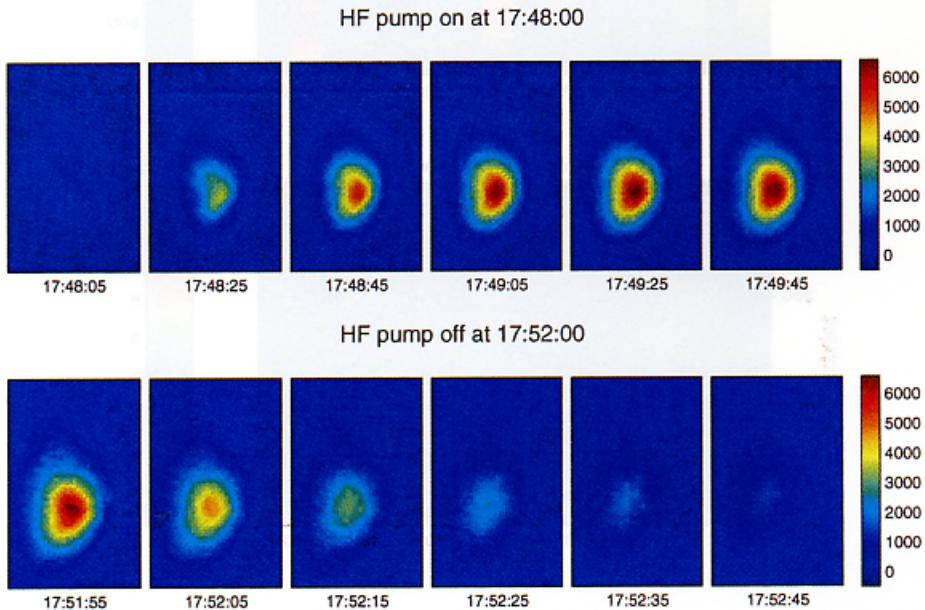
HF pump on at 17:48:00

HF pump off at 17:52:00

Fig. 3. *A series of images of enhanced airglow at 6300 Å near pump-on and -off recorded from the Silkkimuotka station for the pump period 1748–1752 UT. The intensity scale is in raw counts.*
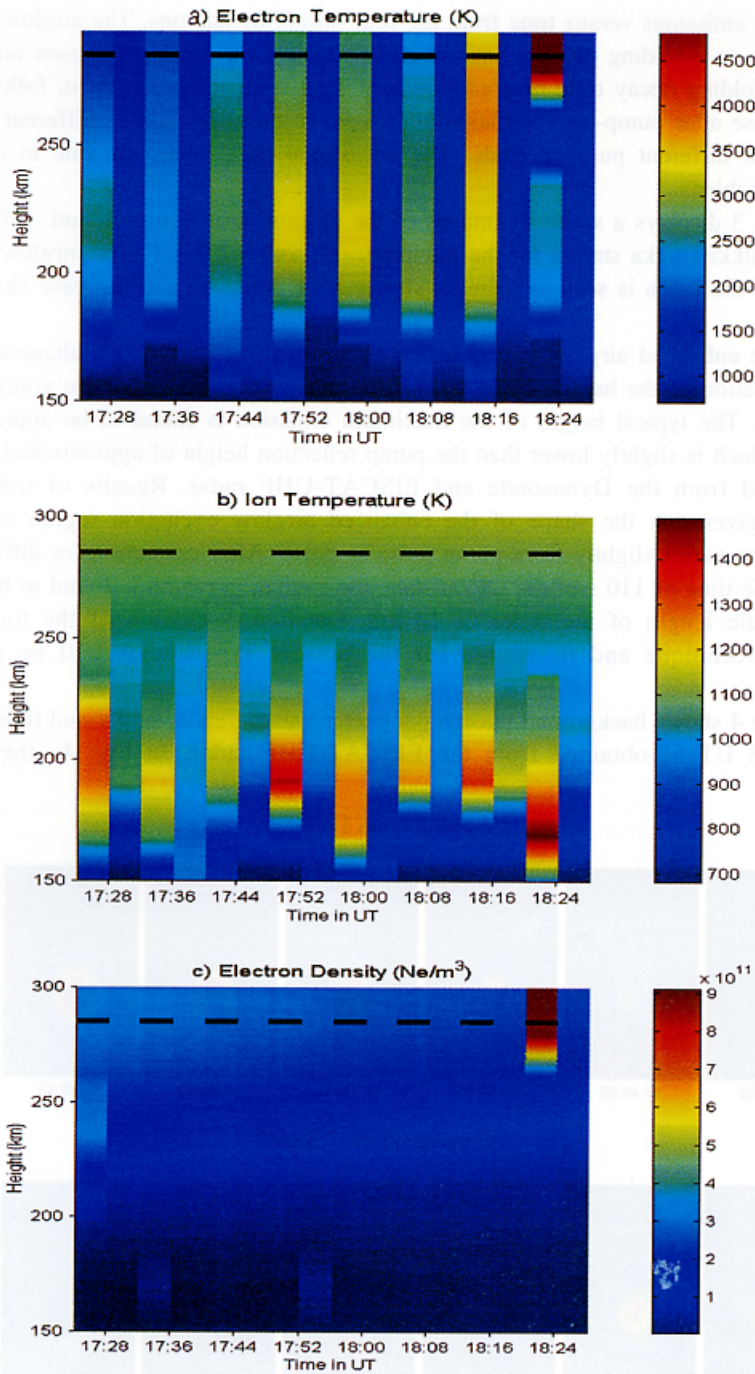
Fig. 4. *The ionospheric electron temperature (a), ion temperature (b), and electron density (c) versus height and time between 1724–1828 UT. The measurements were made with the EISCAT-UHF incoherent scatter radar.*

temperature is shown. Pump-enhanced electron temperature is clearly seen during the pump cycle 4 min on/4 min off. The electron temperature reaches up to approximately 3500 K, which corresponds to an enhancement of 250% of the unperturbed temperature of about 1000 K. The measurement of the very high temperature during the pump period at 1820–1824 UT, as well as the other displayed results in Fig. 4 for the same period, may be contaminated by pump-enhanced ion lines. Further, the temperature enhancements extend several tens of kilometers below and up to 600 km altitude which is several hundreds kilometers above the pump reflection height of approximately 250 km, although Fig. 4a only displays the temperature up to 300 km. As seen in Fig. 4b, the ion temperature is less enhanced than the electron temperature, with the relative temperature enhancements up to approximately 55% of the unperturbed temperature of about 900 K. The maximum ion temperature generally appears to occur at a lower altitude than that where the maximum electron temperature occurs. In Fig. 4c the ionospheric electron density is seen to slowly decay, as expected after the sunset. Since no pump-correlated modulations are seen in the electron density, any large-scale density perturbations are less than approximately 6%.

4. Discussion

Airglow was observed to be weakly enhanced as the HF pump wave was cycled 2 min on/2 min off and significantly more enhanced as the pump cycle was changed to 4 min on/4 min off. Brändström et al. (1999) stated that no enhanced airglow was observed during the 2-min pump periods. However, more detailed analysis has revealed weak airglow enhancements during these periods. Between 1630–1730 UT, as the pump was cycled 2 min on/2 min off, the pump–plasma interaction height varied between 222–240 km. In this case the pump frequency was very close to and slightly below the third multiple of the ionospheric electron gyro frequency in the interaction region, which may have suppressed the temperature enhancement and possibly also the airglow enhancement compared to that observed later during the 4-min pump periods. This is obtained by comparing the pump–plasma interaction height given by the EISCAT-UHF radar with the IGRF model for the geomagnetic field. A minimum in the temperature enhancement during HF pumping has previously been observed for pump frequencies near an electron gyro harmonic, also by using the EISCAT-UHF radar (Honary et al., 1995; Robinson et al., 1996). After 1730 UT the interaction height increased sharply due to changes in the background ionosphere, so that the pump frequency was well above the third electron gyro harmonic. In future experiments it is important to investigate the airglow enhancement for different pump frequencies near a harmonic of the electron gyro frequency. Particularly, in such experiments the effects of upper hybrid and Langmuir turbulence for electron energization and associated airglow enhancements can be discriminated.

Figure 2 shows the temporal evolution of the enhanced airglow intensity for the pump cycling 4 min on/4 min off. The life time of the $O(^1D)$ meta-stable state is approximately 110 s (Solomon et al., 1988), which is significantly longer than the observed decay time of the airglow intensity after pump-off. However, the effective life time of the $O(^1D)$ state at 240-km altitude is reduced due to collisional quenching by

excitation of vibrational states in N_2 and O_2 to as low as 30 s (Sipler and Biondi, 1972). The experimentally determined decay time of 35 s for the enhanced airglow is thus consistent with the effective life time of the $O(^1D)$ state being reduced by quenching. The measured values of the effective life time of the $O(^1D)$ state in HF pump experiments at auroral latitudes may be useful also for studies of the thermosphere and the aurora.

The temporal evolution of the maximum emission intensity in Fig. 2 varies from pump period to period. This indicates that the excitation mechanism for airglow enhancement is not saturated. As seen in Fig. 3, a single patch of enhanced airglow formed. During the previous pump period 1740–1744 UT two airglow patches formed (Brändström *et al.*, 1999). This variability may be a result of natural large-scale plasma density irregularities in the pump–plasma interaction region.

Results from tomography inversion gives that the *e*-folding extent of the airglow excitation region is approximately 10 km. For comparison, the 3-dB width of the pump beam is approximately 15°, which corresponds to a diameter of approximately 60 km at 240-km altitude where the airglow volume emission intensity is maximum. The enhanced airglow cloud is thus significantly smaller than the cross section of the pump beam, which may be a result of that the airglow is enhanced only where the pump wave is the strongest.

The mean free path of electrons having an energy of 3.5 eV parallel to the geomagnetic field near 240 km altitude is 5–10 km. This estimate was obtained by taking the neutral densities from the MSISE-90 model (Hedin, 1991) for an altitude of 240 km and the electron collision cross sections for N_2, O, and O_2 (electron collision cross sections for other species are very small) (Rees, 1989). The size of the airglow excitation region is thus of the same order as the mean free path of energetic electrons along the geomagnetic field which could cause the airglow.

Figure 4 shows background plasma parameter values measured with the EISCAT-UHF incoherent scatter radar. The electron temperature (Fig. 4a) reaches up to 3500 K or 0.3 eV, which may be compared with the effective threshold for exciting the $O(^1D)$ state of approximately 3.5 eV. The maximum temperature enhancement is approximately 250% of the unperturbed temperature. For comparison, the electron temperature during daytime experiments is typically enhanced by a few tens of percent of the unperturbed temperature in high latitude experiments (Jones *et al.*, 1986; Robinson, 1989).

The temperature enhancements extend several tens of kilometers below and several hundreds of kilometers above the pump–ionosphere interaction region of typically a few kilometers height extent near the pump reflection height. This asymmetry is consistent with that the energy input from the relatively narrow pump–ionosphere interaction region is transported mainly upward into the diffusion dominated upper F region while in the collision dominated lower F and E regions the energy is instead lost to the neutrals (Robinson, 1989). This is a result of that the electron–neutral collisions follow the neutral density, which decreases with increasing height.

In daytime experiments it has been found that large scale pump-induced temperature changes as measured with the EISCAT-UHF radar are strongly dependent on anomalous absorption (Honary *et al.*, 1995; Robinson *et al.*, 1996). This has been taken as evidence of that anomalous heating dominates over collisional heating and that it is due to anomalous absorption in high latitude experiments. Anomalous absorption has been

attributed to the excitation of upper hybrid turbulence and the associated formation of magnetic field-aligned density and temperature irregularities (Robinson, 1989; Gurevich *et al.*, 1996). If the large temperature enhancements obtained in the presently discussed nighttime conditions also would be due to anomalous absorption, *i.e.*, due to the excitation of upper hybrid turbulence, then the Langmuir turbulence driven by the parallel pump electric field just below the reflection height would be very weak because of the strong absorption of the pump wave already in the upper hybrid resonance region a few kilometers below the pump reflection height. It is therefore reasonable to expect that the airglow is enhanced by upper hybrid turbulence, which involves electron dynamics essentially perpendicular to the geomagnetic field, and not by Langmuir turbulence, which involves electron dynamics mainly parallel to the geomagnetic field. This is different from the airglow enhancement observed in the mid latitude experiments at Arecibo which has been attributed to Langmuir turbulence (Haslett and Megill, 1974; Sipler *et al.*, 1974; Weinstock, 1975; Gurevich *et al.*, 1985; Bernhardt *et al.*, 1989b). Further experimental work is needed to determine the actual mechanism for the airglow enhancement.

Large HF pump-induced electron temperature enhancements of 1000–2000 K together with ion temperature enhancements of 50–300 K during nighttime have also been reported from experiments at Arecibo (Djuth *et al.*, 1987). The temperature enhancements were correlated with the occurrence of large density cavities with density reductions of 10–15%. The pump wave at 3.175 MHz was transmitted at about 80 MW ERP and reflected at approximately 300 km altitude near the *F*-region peak. Further, the density cavities and temperature enhancements have been associated with large airglow enhancements (Bernhardt *et al.*, 1989a). The presently discussed large electron temperature enhancements and airglow is not associated with any significant density perturbation (Fig. 4c), which is different from the Arecibo results. The reason for this difference is presently not understood. However, it has been proposed that the large cavities and large temperature enhancements in the Arecibo experiments are formed when the maximum ionospheric plasma frequency is relatively low such as in the winter ionosphere during solar minimum conditions, because electrons are less efficiently cooled in the lower density plasmas at higher altitudes (Newman *et al.*, 1988). The presently discussed high latitude experiments were performed in February 1999, which was near solar maximum. However, the used pump frequency of 4.04 MHz was rather low, so that the plasma densities in the interaction region too were rather low. Further, the used ERP was higher but the interaction height of 240 km was lower than in the Arecibo experiments.

5. Conclusion

Enhanced airglow at 6300 Å has been observed by HF-pumping the ionospheric *F*-region plasma at auroral latitudes from the EISCAT-Heating transmitter at Ramfjordmoen in northern Norway. The airglow was detected simultaneously by up to four imaging stations of ALIS in northern Sweden. The multi-station imaging technique enables triangulation of the height and position of the airglow cloud. Further, results of tomography inversion of the imaging data suggest that the shape of the airglow excitation

region is roughly spherical with an *e*-folding scale length of the order of 10 km. The airglow enhancement is correlated with the occurrence of pump-induced electron temperatures up to 3500 K, corresponding to enhancements of 250% of the unperturbed temperature, as measured with the EISCAT-UHF incoherent scatter radar. The temperature enhancements extend several tens of kilometers below and several hundreds of kilometers above the airglow cloud. The high anomalous absorption of the pump wave that is expected for the large electron temperature enhancements suggests that the enhanced airglow is due to upper hybrid turbulence.

Acknowledgments

References

Adeishvili, T. G., Gurevich, A. V., Lyakhov, S. B., Managadze, G. G., Milikh, G. M. and Shlyuger, I. S. (1978): Ionospheric emission caused by an intense radio wave. Sov. J. Plasma Phys., **4**, 721–726.

Bernhardt, P. A., Duncan, L. M. and Tepley, C. A. (1989a): Heater-induced cavities as optical tracers of plasma drifts. J. Geophys. Res., **94**, 7003–7010.

Bernhardt, P. A., Tepley, C. A. and Duncan, L. M. (1989b): Airglow enhancements associated with plasma cavities formed during ionospheric heating experiments. J. Geophys. Res., **94**, 9071–9092.

Bernhardt, P. A., Scales, W. A., Grach, S. M., Keroshtin, A. N., Kotik, D. S. and Polyakov, S. V. (1991): Excitation of artificial airglow by high power radio waves from the "Sura" ionospheric heating facility. Geophys. Res. Lett., **18**, 1477–1480.

Brändström, B. U. E., Leyser, T. B., Steen, Å., Rietveld, M. T., Gustavsson, B., Aso, T. and Ejiri, M. (1999): Unambiguous evidence of HF pump-enhanced airglow at auroral latitudes. Geophys. Res. Lett., **26**, 3561–3564.

Carlson, H. C., Wickwar, V. B. and Mantas, G. P. (1982): Observations of fluxes of suprathermal electrons accelerated by HF excited instabilities. J. Atmos. Terr. Phys., **44**, 1089–1100.

Djuth, F. T., Thidé, B., Ierkic, H. M. and Sulzer, M. P. (1987): Large F-region electron-temperature enhancements generated by high-power HF radio waves. Geophys. Res. Lett., **14**, 953–956.

Gurevich, A. V. and Milikh, G. M. (1997): Artificial airglow due to modifications of the ionosphere by powerful radio waves. J. Geophys. Res., **102**, 389–394.

Gurevich, A. V., Dimant, Y. S., Milikh, G. M. and Vaskov, V. V. (1985): Multiple acceleration of electrons in the regions of high-power radio-wave reflection in the ionosphere. J. Atmos. Terr. Phys., **47**, 1057–1070.

Gurevich, A. V., Lukyanov, A. V. and Zybin, K. P. (1996): Anomalous absorption of powerful radio waves on the striations developed during ionospheric modification. Phys. Lett. A, **211**, 363–372.

Haslett, J. C. and Megill, L. R. (1974): A model of the enhanced airglow excited by RF radiation. Radio Sci., **9**, 1005–1019.

Hedin, A. E. (1991): Extension of the MSIS thermosphere model into the middle and lower atmosphere. J. Geophys. Res., **96**, 1159–1172.

Honary, F., Stocker, A. J., Robinson, T. R., Jones, T. B. and Stubbe, P. (1995): Ionospheric plasma response to HF radio waves operating at frequencies close to the third harmonic of the electron gyrofrequency. J. Geophys. Res., **100**, 21489–21501.

Jones, T. B., Robinson, T. R., Stubbe, P. and Kopka H. (1986): EISCAT observations of the heated ionosphere. J. Atmos. Terr. Phys., **48**, 1027–1035.

Leyser, T. B. (1991): Parametric interaction between upper hybrid and lower hybrid waves in heating experiments. Geophys. Res. Lett., **18**, 408–411.

Mantas, G. P. (1994): Large 6300-Å airglow intensity enhancements observed in ionospheric heating experiments are excited by thermal electrons. J. Geophys. Res., **99**, 8993–9002.

Mantas, G. P. and Carlson, H. C. (1996): Reinterpretation of the 6300-Å airglow enhancements observed in ionospheric heating experiments based on analysis of Platteville, Colorado, data. J. Geophys. Res., **101**, 195–209.

Newman, A. L., Carlson, H. C., Jr., Mantas, G. P. and Djuth, F. T. (1988): Thermal response of the F-region ionosphere for conditions of large HF-induced electron-temperature enhancements. Geophys. Res. Lett., **15**, 311–314.

Perkins, F. W. and Kaw, P. K. (1971): On the role of plasma instabilities in ionospheric heating by radio waves. J. Geophys. Res., **76**, 282–284.

Rees, M. H. (1989): Physics and Chemistry of the Upper Atmosphere. New York, Cambridge University Press, 271–277.

Rietveld, M. T., Kohl, H., Kopka, H. and Stubbe, P. (1993): Introduction to ionospheric heating at Tromsø–I. Experimental overview. J. Atmos. Terr. Phys., **55**, 577–599.

Robinson, T. R. (1989): The heating of the high latitude ionosphere by high power radio waves. Phys. Rep., **179**, 79–209.

Robinson, T. R., Honary, F., Stocker, A. J., Jones, T. B. and Stubbe, P. (1996): First EISCAT observations of the modification of F-region electron temperatures during RF heating at harmonics of the electron gyro frequency. J. Atmos. Terr. Phys., **58**, 385–395.

Sipler, D. P. and Biondi, M. A. (1972): Measurements of $O(^1D)$ quenching rates in the F region. J. Geophys. Res., **77**, 6202–6212.

Sipler, D. P., Enemark, E. and Biondi, M. A. (1974): 6300-Å intensity variations produced by the Arecibo ionospheric modification experiment. J. Geophys. Res., **79**, 4276–4280.

Solomon, S. C., Hays, P. B. and Abreu, V. J. (1988): The auroral 6300 Å emission: Observations and modeling. J. Geophys. Res., **93**, 6867–6882.

Steen, Å. and Brändström, U. (1993): A multi station ground-based imaging system at high latitudes. STEP International Newsletter, **3**, 11–14.

Wannberg, G. (1993): The G2-system and general purpose alternating code experiments for EISCAT. J. Atmos. Terr. Phys., **55**, 543–557.

Weinstock, J. (1975): Theory of enhanced airglow during ionospheric modifications. J. Geophys. Res., **80**, 4331–4345.